Three Nucleon Force Effects in Intermediate Energy Deuteron Analyzing Powers for dp Elastic Scattering

K. Sekiguchi[1],* H. Okamura[2],† N. Sakamoto[3], H. Suzuki[4], M. Dozono[5], Y. Maeda[6],
T. Saito[6], S. Sakaguchi[3], H. Sakai[3,7], M. Sasano[3], Y. Shimizu[8], T. Wakasa[5],
K. Yako[7], H. Witała[9], W. Glöckle[10], J. Golak[9], H. Kamada[11], and A. Nogga[12]

[1]*Department of Physics, Tohoku University, Sendai, 980-8578, Japan*
[2]*Research Center for Nuclear Physics, Osaka University, Ibaraki, Osaka, 567-0047, Japan*
[3]*RIKEN Nishina Center, Wako, 351-0198, Japan*
[4]*Graduate School of Pure and Applied Sciences, University of Tsukuba, Tsukuba, 305-8571, Japan*
[5]*Department of Physics, Kyushu University, Fukuoka, 812-8581, Japan*
[6]*Faculty of Engineering, University of Miyazaki, Miyazaki, 889-2192, Japan*
[7]*Department of Physics, University of Tokyo, Tokyo, 113-0033, Japan*
[8]*Center for Nuclear Study, University of Tokyo, Tokyo, 113-0033, Japan*
[9]*Institute of Physics, Jagiellonian University, PL-30059 Cracow, Poland*
[10]*Institut für theoretische Physik II, Ruhr-Universität Bochum, D-44780 Bochum, Germany*
[11]*Department of Physics, Kyushu Institute of Technology, Kitakyushu 804-8550, Japan and*
[12]*Institut für Kernphysik, Institute for Advanced Simulation and Jülich Center for Hadron Physics, D-52428 Jülich, Germany*
(Dated: June 18, 2013)

A complete high precision set of deuteron analyzing powers for elastic deuteron-proton (dp) scattering at 250 MeV/nucleon (MeV/N) has been measured. The new data are presented together with data from previous measurements at 70, 100, 135 and 200 MeV/N. They are compared with the results of three-nucleon (3N) Faddeev calculations based on modern nucleon-nucleon (NN) potentials alone or combined with two models of three nucleon forces (3NFs): the Tucson-Melbourne 99 (TM99) and Urbana IX. At 250 MeV/N large discrepancies between pure NN models and data, which are not resolved by including 3NFs, were found at c.m. backward angles of $\theta_{\text{c.m.}} \gtrsim 120°$ for almost all the deuteron analyzing powers. These discrepancies are quite similar to those found for the cross section at the same energy. We found small relativistic effects that cannot resolve the discrepancies with the data indicating that other, short-ranged 3NFs are required to obtain a proper description of the data.

A hot topic in present day few-nucleon system studies is exploring the properties of three-nucleon forces (3NFs) that appear when more than two nucleons ($A \geq 3$) interact. The 3NFs arise naturally in the standard meson exchange picture in which the main ingredient is considered to be 2π-exchange between three nucleons along with the Δ–isobar excitation, the mechanism initially proposed a half century ago by Fujita and Miyazawa [1]. Further enhancements have led to the Tucson–Melbourne (TM) [2] and Urbana IX 3NF [3] models. New impetus to study 3NFs has come from chiral effective field theory (χEFT) descriptions of nuclear interactions. In that framework consistent two-, three-, and many-nucleon forces are derived on the same footing [4, 5]. The first non-zero contribution to 3NFs appears in χEFT at the next-to-next-to-leading order (N²LO) of the chiral expansion. That explains why 3NFs are relatively small compared to NN forces (2NFs) and why their effects are easily masked. Therefore, it is, in general, hard to find evidence for them.

The first evidence for a 3NF was found in the three-nucleon bound states, ³H and ³He [9, 10]. The binding energies of these nuclei are not reproduced by exact solutions of three-nucleon Faddeev equations employing modern NN forces only, *i.e.* AV18 [6], CD Bonn [7], Nijmegen I, II and 93 [8]. The underbinding of ³H and ³He can be explained by adding a 3NF, mostly based on 2π-exchange, acting between three nucleons [9–11]. The importance of 3NFs has been further supported by the binding energies of light mass nuclei. *Ab initio* microscopic calculations of light mass nuclei, such as Green's Function Monte Carlo [12] and no-core shell model calculations [13], highlight the necessity of including 3NFs to explain the binding energies and low-lying levels of these nuclei.

In addition to the study of 3N bound states, three nucleon scattering is an attractive candidate for a further, more detailed investigation of properties of 3NFs, such as their momentum, spin, and/or isospin dependence. In elastic nucleon-deuteron (Nd) scattering and in deuteron breakup reactions one can measure not only differential cross sections but also a rich set of polarization observables under various kinematic conditions. The importance of 3NFs in Nd elastic scattering was shown for the first time in [14]. Clear signals from 3NFs were found around the cross section minimum occurring at c.m. angle $\theta_{c.m.} \approx 120°$ for incident energies above 60 MeV/N. Since then experimental studies of proton–deuteron (pd)

and/or neutron–deuteron (nd) elastic scattering at intermediate energies have been performed extensively and have provided precise data for cross sections [15–21] and spin observables, such as analyzing powers [15–19, 21–24], spin correlation coefficients [24], and polarization transfer coefficients [18, 25, 26]. Large discrepancies between data and rigorous Faddeev calculations with modern NN forces alone have been reported, which are particularly significant in the angular region of the cross section minimum and at incident nucleon energies above about 60 MeV/N. In the case of the cross sections, a larger part of the discrepancies are removed combining the NN forces with a 3NF such as the TM99 [27] or Urbana IX. Those results can be taken as clear signatures for 3NF effects in Nd elastic scattering and the data themselves form a solid basis to test new theories. In contrast to the elastic scattering cross section the theoretical predictions with 3NFs included still have difficulties in reproducing data for some spin observables.

In Refs. [18, 21], precise data for the cross section and nucleon analyzing powers at 250 MeV/N in pd and nd elastic scattering were reported. Contrary to the results obtained at lower energies, the discrepancies in the cross sections were only partially removed by incorporating 3NFs and large discrepancies of $\approx 40\%$ still remained at backward angles $\theta_{\mathrm{c.m.}} \gtrsim 120°$.

The results of Refs. [18, 21] present a new challenge to be solved and show that an energy dependent study of a variety of spin observables should be a good source to obtain a consistent understanding of the dynamics of nuclear forces in elastic Nd scattering. Especially the deuteron tensor analyzing powers should be interesting, because matrix elements of the 2π-exchange 3NF consist of momentum-spin coupled operators. Data for the cross section and spin observables in elastic pd/nd scattering have been accumulated at incident energies $\lesssim 200$ MeV/N. However, only a few precise data exist around 200–300 MeV/N. The new accelerator facility at RIKEN, RI beam factory (RIBF), where polarized deuteron beams are available up to 440 MeV/N, offers opportunities to make these experimental studies. As the first experiment with a vector and tensor polarized deuteron beam at RIBF, the measurement of elastic dp scattering at 250 MeV/N was performed, providing a complete set of data for all deuteron analyzing powers iT_{11}, T_{20}, T_{21} and T_{22}, in a wide angular range $\theta_{\mathrm{c.m.}} = 36°$–$162°$.

At RIBF the vector and tensor polarized deuteron beam was accelerated first by the injector cyclotrons AVF and RRC up to 90 MeV/N, and then up to 250 MeV/N by the new superconducting cyclotron SRC. The measurement of elastic dp scattering was performed with the new beam line polarimeter BigDpol, installed at the extraction beam line of the SRC. A polyethylene (CH_2) target with a thickness of 330 mg/cm^2 was used as a hydrogen target. In the BigDpol four pairs of plastic scintillators coupled with photo-multiplier tubes were mounted in two independent planes, 90° apart in azimuthal angle and

operated in kinematic coincidence for elastic dp scattering. The opening angle of the BigDpol was 8°–70°. The solid angles were determined by the proton detectors and the angular spread was $\Delta\theta_{\mathrm{lab.}} \pm 1°$. For subtraction of events from the proton knock-out reaction on carbon nuclei $^{12}\mathrm{C}(d,dp)^{11}\mathrm{B}$ a measurement with a graphite target was also performed.

The data were taken with polarized and unpolarized beams for different combinations of the incoming polarization given in terms of the theoretical maximum polarization values as $(p_Z, p_{ZZ}) = (0,0)$, $(1/3,-1)$, $(-2/3,0)$ and $(1/3,1)$. Those polarization modes were changed cyclically at intervals of 5 seconds by switching the RF transition units of the polarized ion source. The beam polarizations were monitored continuously with a beam line polarimeter prior to acceleration by the SRC using elastic dp scattering at 90 MeV/N. The analyzing powers for this reaction were calibrated in the previous measurement by using the $^{12}\mathrm{C}(d,\alpha)^{10}\mathrm{B}^*[2^+]$ reaction, the $A_{zz}(0°)$ of which is exactly -1 because of parity conservation [29]. In the present measurement typical values of the beam polarizations were 80% of the theoretical maximum values.

The deuteron analyzing powers for elastic dp scattering are expressed through the unpolarized (σ_0) and polarized (σ) cross sections together with the vector and tensor polarizations of the incoming deuteron (p_Z and p_{ZZ}) as

$$
\begin{aligned}
\sigma = \sigma_0 \Big\{ &1 + \sqrt{3}\, iT_{11}(\theta)\, p_Z \sin\beta \cos\phi \\
&+ \frac{1}{\sqrt{8}}\, T_{20}(\theta)\, p_{ZZ}\left(3\cos^2\beta - 1\right) \\
&+ \sqrt{3}\, T_{21}(\theta)\, p_{ZZ} \cos\beta \sin\beta \sin\phi \\
&+ \frac{\sqrt{3}}{2}\, T_{22}(\theta)\, p_{ZZ} \sin^2\beta \cos 2\phi \Big\},
\end{aligned} \quad (1)
$$

where θ and ϕ are the polar and azimuthal scattering angles, respectively [30]. The β is defined as the angle between the spin direction and the beam direction. In this experiment the polarization axis of the deuteron beam was rotated with a Wien filter system to the direction required for the measurement of a particular analyzing power [31]. For the measurement of the analyzing powers iT_{11}, T_{20}, and T_{22} the polarization axis was normal to the horizontal plane. For the T_{21} measurement the spin symmetry axis was rotated in the reaction plane and aligned at an angle $\beta = 38.0° \pm 0.51°$ to the beam direction.

Figures 1(a) and (b) show spectra of scintillator light outputs of one pair of the deuteron and proton detectors placed at 19.5° and 55°, respectively. The spectra obtained with the CH_2 target together with the graphite target are shown. Impinging deuterons and protons punched through the detectors. Identification of the scattered deuterons and recoil protons was performed by cuts for the spectrum with the CH_2 target as shown in Figs. 1(a) and (b). After the selection of events a spectrum of the time-of-flight difference between the deuteron

and proton detectors was obtained (see Fig. 1(c)). As for asymmetry determination of elastic dp scattering the selected events within the gate shown in Fig. 1(c) were used. Since the contribution from carbon nuclei was small in Fig. 1(c) the background subtraction was not performed in the analysis.

We present these new data and compare them with theoretical predictions based on different dynamical input in Fig. 2. The statistical uncertainties, which are less than 0.01 for all the deuteron analyzing powers, are also shown. In order to clarify the energy dependence, the previously measured deuteron analyzing powers at 70, 100 and 135 MeV/N [15–17, 25] and at 200 MeV/N [24] are also included together with theoretical predictions. The deuteron analyzing powers at 70, 100, 135 MeV/N have been reported in Refs. [15–17, 25] in the Cartesian notation. Here we show them in the spherical description. The theoretical predictions shown are based on modern NN forces alone and on their combinations with 3NF models [32, 33]. We used high precision NN potentials AV18, CD Bonn, and Nijmegen I and II alone [light shaded (blue) bands in Fig. 2] or combined them with the TM99 3NF [27] with the cutoff Λ values that yield, for a particular NN force and TM99 combination, a reproduction of the ^{3}H binding energy [dark shaded (red) bands in Fig. 2]. In case of the AV18 NN force, we also combined it with the Urbana IX 3NF [3] (solid lines in Fig. 2). In our calculations we neglected the Coulomb force acting between two protons. At energies considered here its effect on polarization observables is small [28].

For the vector analyzing power iT_{11} the predicted 3NF effects at 70 MeV/N are small and the data are satisfactorily described, independently of whether 3NFs are included. At higher energies, however, a discrepancy between data and theory based on NN forces only is clearly seen for c.m. angles $\theta_{c.m.} \gtrsim 80°$. At 100 and 135 MeV/N adding TM99 or Urbana IX 3NF provides quite a good description of the data. That is not the case at 200 and 250 MeV/N, where only a part of the discrepancy is removed and the full theory is quite far from data in some angular regions. For $\theta_{c.m.} \lesssim 60°$ at all energies 3NF effects are negligible and data are reproduced by pure NN theory.

For the tensor analyzing power T_{20}, the predicted 3NF effects are smaller than for iT_{11}. Again, at 70 MeV/N the theory reasonably well reproduces the data and at 100 and 135 MeV/N adding 3NFs brings the theory closer to the data. At 200 and 250 MeV/N, where the predicted 3NF effects for T_{20} are rather moderate, drastic discrepancies between theory and data in the angular region $80° \lesssim \theta_{c.m.} \lesssim 140°$ are clearly seen, which are not explained by adding standard 3NFs.

The data for the tensor analyzing power T_{21} are reproduced quite well by calculations with the 2NFs only for all incident energies. The large effects of the TM99 3NF predicted for energies $\gtrsim 100$ MeV are not supported by the T_{21} data. They differ clearly from the smaller effects of the Urbana IX 3NF, which generally leads to a better
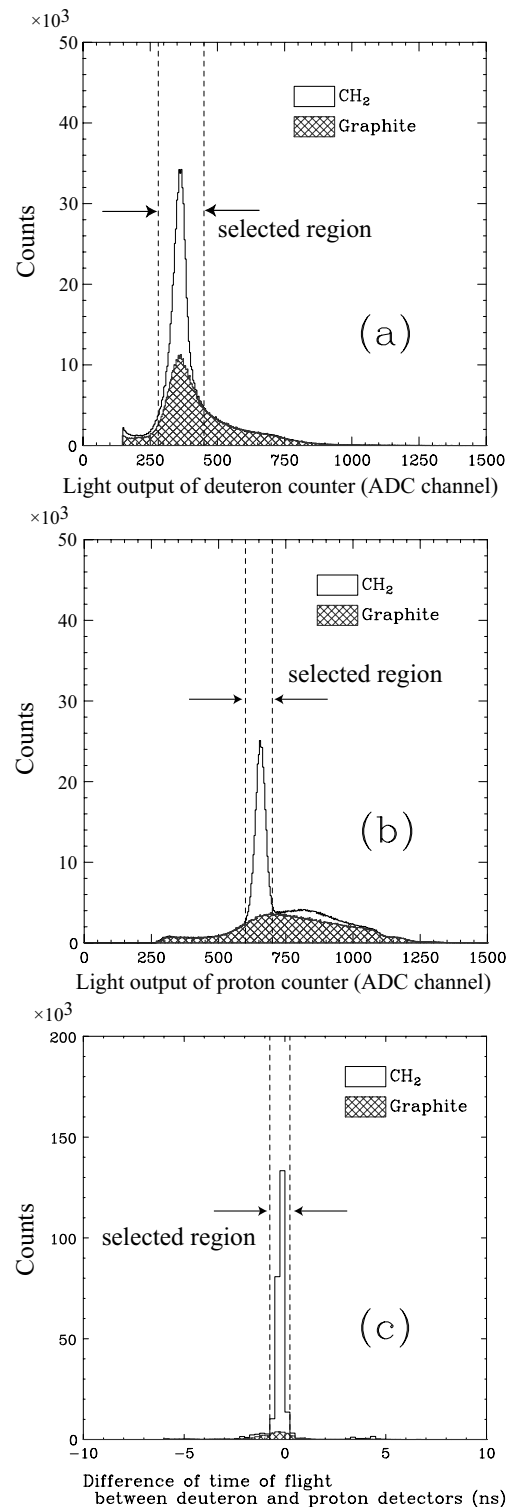

FIG. 1: Spectra of light outputs of of the scintillation counters for the scattered deuterons (a) and the recoil protons (b). The deuteron and proton detectors were placed at $19.5°$ and $55°$, respectively. After selecting events in (a) and (b) the spectra of time of flight difference between the deuteron and proton detectors was obtained (c).
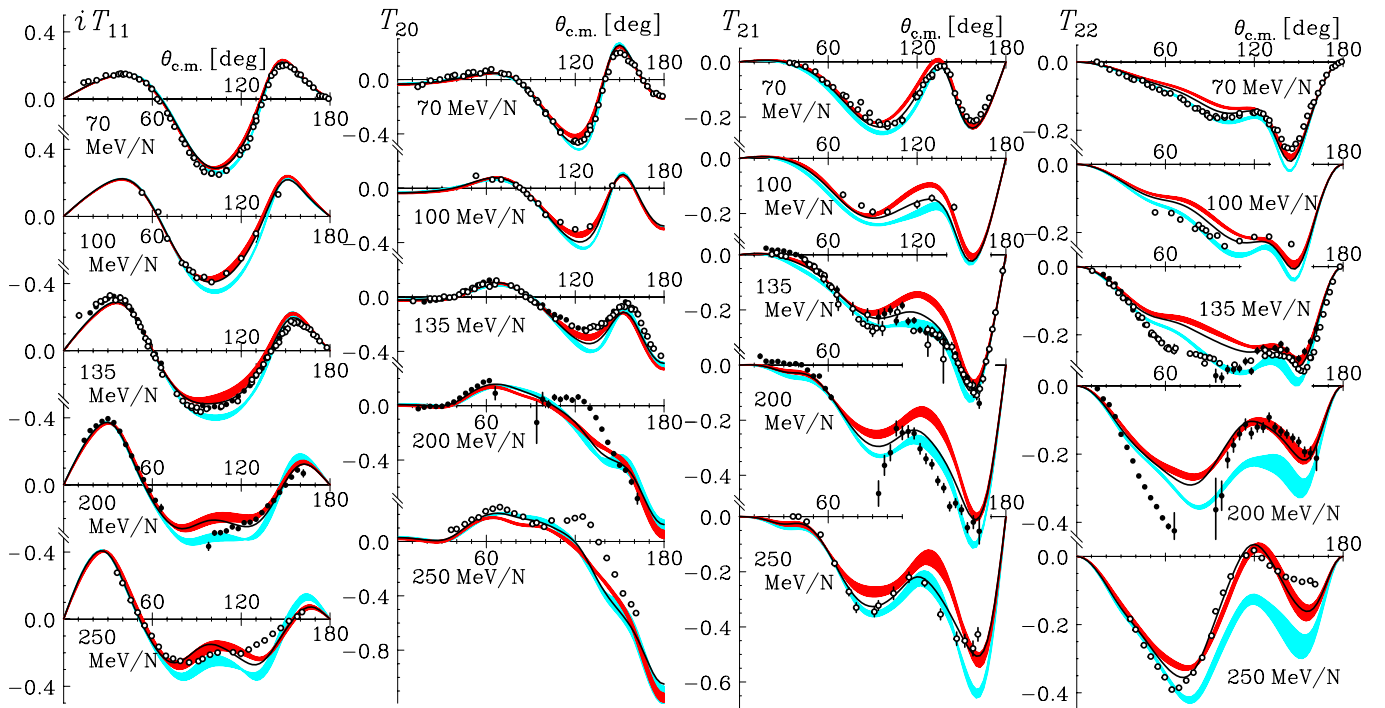
FIG. 2: (Color online) The deuteron analyzing powers iT_{11}, T_{20}, T_{21}, and T_{22} for dp elastic scattering at 70, 100, 135, 200, and 250 MeV/N. The light shaded (blue) bands contain predictions of modern NN potentials: AV18, CD Bonn, Nijmegen I and II. The dark shaded (red) bands result when those potentials are combined with TM99 3NF, properly adjusted to reproduce the ^{3}H binding energy. The solid line is the result obtained with the combination AV18+Urbana IX. The pd data are: at 70 MeV/N (open circles) from Ref. [25], at 100 MeV/N (open circles) from Ref. [17], at 135 MeV/N (open circles) from Ref. [17] and (solid circles) from Ref. [24], at 200 MeV/N (solid circles) from Ref. [24], and at 250 MeV/N (open circles) from the present study.

description for that observable.

For the tensor analyzing power T_{22}, the discrepancies between the data and the predictions based on 2NFs only become larger in magnitude and expand to the backward angles with increasing incident energy. For that observable the predicted 3NF effects are especially large and similar in magnitude for the 2NFs plus TM99 and Urbana IX models. At 200 MeV/N and less the predictions taking into account 3NFs have good agreement to the data at the backward angles, however the data in the angular region $40° \lesssim \theta_{c.m.} \lesssim 120°$ are not described by any theoretical predictions. At 250 MeV/N the overall agreement is improved by taking into account these 3NFs except for the very backward angles.

All the deuteron analyzing powers, with exception of T_{21}, reveal at the highest energy 250 MeV/N and around c.m. angles $\theta_{c.m.} \gtrsim 120°$ large discrepancies to theory based on NN forces alone, which are not resolved completely by the inclusion of the 3NFs. Such behavior of the deuteron analyzing powers is quite similar to that of the cross section and proton/neutron analyzing powers at 250 MeV/N found in Refs. [18, 21].

The energy dependence of the predicted 3NF effects and the difference between the theory and the data for the deuteron analyzing powers is not always similar to that of the cross section and nucleon analyzing power.

The vector analyzing power iT_{11} and the tensor analyzing power T_{20} have features similar to those of the cross section and the proton analyzing power A_y^p. However the tensor analyzing power T_{21} and T_{22} reveal different energy dependence from that of other observables. Starting from ~ 100 MeV/N large 3NF effects are predicted. For T_{21} they are of different magnitude for TM99 and Urbana IX and the T_{21} data seem to prefer the smaller effects of Urbana IX. For T_{22} the large effects of TM99 and Urbana IX are practically the same. At 200 MeV/N and below adding 3NFs worsens the description of data in a large angular region. It is contrary to what happens at the highest energy 250 MeV/N, where large 3NF effects are supported by the T_{22} data in a large angular range.

The results obtained for the highest energy of 250 MeV/N indicate that some significant components are missing in the calculations, especially in the regions of higher momentum transfer. One possible candidate is relativistic effects. We estimated their magnitude for the deuteron tensor analyzing powers by comparing nonrelativistic and relativistic predictions based on the CD Bonn potential [34, 35]. They turned out to be small and only slightly alter the deuteron analyzing powers.

Due to the smallness of the considered relativistic effects, it appears that important parts of the 3NFs are missing. In the meson exchange picture used here, con-

tributions of heavy mesons, e.g. π–ρ and ρ–ρ exchanges are omitted. The importance of such contributions is also seen in χEFT, where the leading non-vanishing 3NF consists of a 2π-exchange, a 1π exchange-contact and a pure contact interaction topology. With increasing energy orders of the chiral expansion higher than N^{2}LO become important, which introduce a multitude of additional short-range 3NF contributions, coming with different momentum-spin dependence. The complicated energy dependence of the deuteron analyzing powers and their strong dependence on the 3NF model used indicates the importance of such short-range components in their full description. The results of Faddeev calculations based on a force model with explicit Δ degrees of freedom show large changes in the predicted analyzing powers [36] and also indicate the importance of short-range 3NF components in the description of these spin observables.

In summary we have reported the first complete set of high precision data for the deuteron analyzing powers iT_{11}, T_{20}, T_{21}, and T_{22}, in elastic dp scattering at 250 MeV/N, taken in a wide angular range $\theta_{\text{c.m.}} = 36°$–$162°$. These data constitute a solid basis to guide theoretical investigations of 3NF models at intermediate energies. It seems that missing short-range 3NF components are necessary in order to achieve a proper description of the data, such as e.g. provided by χEFT. So far the framework of the χEFT is only applicable up to $\sim 100\,\text{MeV/N}$ for 3N scattering. It would be interesting, however, to see in future how converged theoretical predictions based on the χEFT forces describe our data.

[1] J. Fujita and H. Miyazawa, Prog. Theor. Phys. **17**, 360 (1957).
[2] S. A. Coon and W. Glöckle, Phys. Rev. C**23**, 1790 (1981).
[3] B. S. Pudliner et al., Phys. Rev. C**56**, 1720 (1997).
[4] U. van Kolck, Phys. Rev. C **49**, 2932 (1994).
[5] E. Epelbaum, H.-W. Hammer, U.-G. Meißner, Rev. Mod. Phys. **81**, 1773 (2009).
[6] R. B. Wiringa et al., Phys. Rev. C **51**, 38 (1995).
[7] R. Machleidt, Phys. Rev. C **63**, 024001 (2001).
[8] V. G. J. Stoks et al., Phys. Rev. C **49**, 2950 (1994).
[9] C. R. Chen et al., Phys. Rev. C**33**, 1740 (1986).
[10] T. Sasakawa and S. Ishikawa, Few-Body Syst. **1**, 3 (1986).
[11] A. Nogga et al., Phys. Rev. C**65**, 054003 (2002).
[12] S. C. Pieper et al., Phys. Rev. C **66**, 044310 (2002).
[13] P. Navrátil and W.E. Ormand, Phys. Rev. C **68**, 034305 (2003).
[14] H. Witała et al., Phys. Rev. Lett. **81**, 1183 (1998).
[15] N. Sakamoto et al., Phys. Lett. B **367**, 60 (1996).
[16] H. Sakai et al., Phys. Rev. Lett. **84**, 5288 (2000).
[17] K. Sekiguchi et al., Phys. Rev. C **65**, 034003 (2002).
[18] K. Hatanaka et al., Phys. Rev. C **66**, 044002 (2002).
[19] K. Ermisch et al., Phys. Rev. C **71**, 064004 (2005).
[20] K. Sekiguchi et al., Phys. Rev. Lett. **95**, 0162301 (2005).
[21] Y. Maeda et al., Phys. Rev. C **76**, 014004 (2007).
[22] E. J. Stephenson et al., Phys. Rev. C **60**, 061001 (1999).
[23] R. Bieber et al., Phys. Rev. Lett. **84**, 606 (2000).
[24] B. v. Przewoski et al., Phys. Rev. C **74**, 064003 (2006).
[25] K. Sekiguchi et al., Phys. Rev. C **70**, 014001 (2004).
[26] H. R. Amir-Ahmadi et al., Phys. Rev. C **75**, 041001 (2007).
[27] S.A. Coon, H.K. Han, Few Body Syst., **30**, 131 (2001).
[28] A. Deltuva, A.C. Fonseca, P.U.Sauer, Phys. Rev. C **72**, 054004 (2005).
[29] H. Mardanpour et al., Eur. Phys. J. A **31**, 383 (2007).
[30] G. G. Ohlsen, Rep. Prog. Phys. **35**, 717 (1972).
[31] H. Okamura et al., AIP Conf. Proc. **343**, 123 (1995).
[32] W. Glöckle et al., Phys. Rep. **274**, 107 (1996).
[33] D. Hüber et al., Acta Phys. Polonica B **28**, 1677 (1997).
[34] H. Witała et al., Phys. Rev. C **71**, 054001 (2005).
[35] H. Witała et al., Phys. Rev. C **77**, 034004 (2008).
[36] A. Deltuva, private communication.